Science and Technology Indonesia
e-ISSN:2580-4391 *p*-ISSN:2580-4405
Vol. 8, No. 4, October 2023

Research Paper

Spectroscopic Diagnostics of Spectral Lines Emission from Cu Plasma within the Visible Spectrum Range

Hayim Ch. Magid[1*], Bushra Khamas Abbas[2], Dunia F. T. AL-Ani[2]

[1]*Department of Physics, College of Education, Mustanseriyah University, Baghdad, 10052, Iraq*
[2]*Department of Physics, College of Science, Mustansiriyah University, Baghdad, 10052, Iraq*
***Corresponding author**: halhelfy@yahoo.com / halhelfy@uomustansiriyah.edu.iq

Abstract
The creation and characterization of laser-induced plasma (LIP), a significant phenomenon in several applications, are influenced by the sample's physical qualities as well as the laser's parameters. In this research, we created Cu plasma in the atmosphere using an Nd: YAG laser operating at a wavelength of 532 nm with a laser irradiance energy range (400-800) mJ. The effect of the laser's irradiance energy on the plasma characteristics was investigated using optical emission spectroscopy (OES). Using the two ratio and Stark broadening methods, we successfully measured the two most important plasma properties (electron temperature and electron density). The electron's plasma temperature value ranged from 2.3 to 3 eV. The value of electron plasma density is in the range from 6.75×10^{17} to 15×10^{17} cm^{-3}. Also, we found that other plasma parameters like plasma frequency (f_p), particles in the Debye sphere (N_D), and Debye length (λ_D) are affected by laser energy. Where plasma frequency ranged from 7.378 to 10.998×10^{12} Hz, the Debye sphere ranged from 7.294 to 7.022×10^{3}, and the range of Debye length from 1.372 to 1.038×10^{-5} cm.

Keywords
Cu Plasma, Laser Irradiance, Boltzmann Plot, Two Line Ratio, Plasma Parameters

Received: 21 February 2023, Accepted: 7 August 2023
https://doi.org/10.26554/sti.2023.8.4.710-715

1. INTRODUCTION

Using a pulsed-intensity laser to cause a controlled chemical reaction is the basis of laser-induced breakdown spectroscopy (LIBS), an analytical method. This laser can be focused on the surface of the sample, ablating and exciting a very small amount of material (Li et al., 2019; Botto et al., 2019). While in the state of plasma, the ablated material produces a spectrum that is unique to it. The chemical components of the sample are revealed in both qualitative and quantitative detail by this spectrum (Botto et al., 2019; Keerthi et al., 2022). Plasma contains excited atoms and ions that produce radiation when they relax to the ground energy level (Radziemski, 2002). Recent studies have examined optical emission from laser-generated plasmas and calculated atomic and ionic line emission utilizing laser interaction with the sample target (Bulajic et al., 2002).

Analyzing plasma emissions using a spectrometer reveals element identities and concentrations. Estimating plasma properties like electron temperature and density may diagnose plasma (Mohammed et al., 2022b). One of the past century's most rapidly expanding analytical methods is laser-induced breakdown spectroscopy (LIBS) due to its speed, mobility, the capacity of in situ remote analysis without sample treatment, and simplicity of use (Botto et al., 2019). LIBS technique has been used effectively in a wide variety of domains, including bio-medicine (Corsi et al., 2003; Sancey et al., 2014; Pyun et al., 2023), environmental protection (Yamamoto et al., 1996; Kasem et al., 2011; Tavares et al., 2022), industrial diagnostics (Lorenzetti et al., 2015), forensic investigation (Gupta et al., 2017), etc. LIBS technique characteristics depend on laser parameters (energy, pulse duration, and wavelength), sample characteristics (optical absorption coefficient, thermal conductivity, melting and boiling point thermal diffusivity, surface reflectivity), ablated material amount, and atmospheric environmental composition (Shaikh et al., 2008).

Many experimental investigations have examined the influence of the factors above on LIBS analytical performance. Afgan et al. (2018) used an Nd: YAG laser set to 1064 nm to do a spectroscopic analysis of thallium plasma. They reported that laser irradiance had been used to measure plasma temperature and electron density. The influence of Nd: YAG laser intensity and wavelength on the plasma characteristics of emission Magnesium lines is investigated by (Mohammed et al., 2022a). When comparing the fundamental laser (1064 nm) and the second harmonic (532 nm) cases, plasma temperatures are greater in the former. This research aimed to examine

Table 1. Cu Plasma Spectral Line Emission Spectroscopy Parameters Related to the NIST Database (NIST)

Spectral lines	λ (nm)	$g_i A_{ij}$ (s^{-1})	E_j (eV)
Cu I	570	9.60×10^5	3.816
Cu II	593.76	7×10^7	17.21

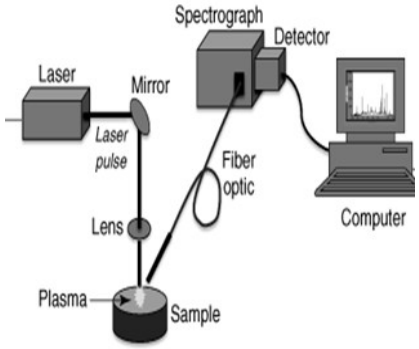

Figure 1. LIBS System Diagram Experiential to Generate Cu Plasma

how changing the laser energy affected the spectral lines and characteristics of Cu plasma at the visible spectrum range.

2. EXPERIMENTAL SECTION

Figure 1 depicts the experimental setup for laser-induced breakdown spectroscopy (LIBS). In this experiment, a nanosecond Q-switched Nd: YAG laser set to 532 nm wavelength, 6 Hz in repetition frequency, 10 ns in pulse duration, and laser energy from 400 to 800 mJ is used to generate plasma. The Cu powder was compressed using a hydraulic press at 80 MPa for 10 minutes. At atmospheric pressure, a 10 cm quartz lens focussed the laser beam on the target's surface. A 50 mm diameter optical wire was used to collect the Cu target surface's plasma light. The fiber was elevated 1 cm above the sample and connected to a Surwit (S3000-UV-NIR) spectrometer that was used to study plasma emissions. To analyze the Cu plasma features, the lines spectral emission of Cu plasma were compared with NIST database software (NIST), as shown in Table (1).

3. RESULTS AND DISCUSSION

3.1 Diagnostics of Spectral Lines Emission

Optical emission spectroscopy was used to study the Nd: YAG laser-produced Cu plasma within the visible spectrum range. As laser energy is a factor in plasma emission intensity, its impact on plasma properties was investigated. The ionic and atomic emission spectra of the Cu plasma demonstrate that optical emissions are generated as a result of the decay of excited species in the plasma. The Cu plasma spectra ranged from 550 to 700 nm, with the emission of 7 spectral lines following excitation by the 532 nm wavelength at various laser irradiance energies ranging from 400 to 800 mJ. The spectral

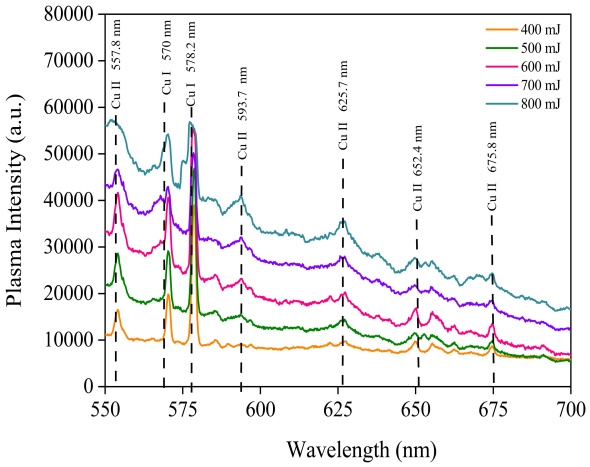

Figure 2. Spectral Lines Emission of Cu Plasma Generated by 532 nm Laser at Various Laser Irradiation Energies

lines emission includes two atomic spectral lines for Zn I at 570 nm and 578.2 nm and five ionic spectral lines for Cu II at 557.8 nm, 593.7 nm, 625.7 nm, 654.4 nm, and 675.8 nm, as shown in Figure 2.

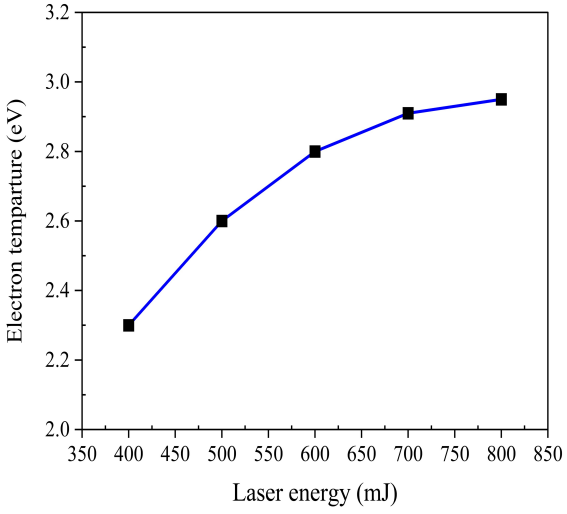

Figure 3. The Electron Plasma Temperature at Different Laser Energy

The intensity of the ionic and atomic emission spectra of Cu plasma increased as the laser irradiance energy increased from 400 mJ to 800 mJ, as shown in Figure 2. Increased laser irradiance energy causes an increase in the plasma's ability to absorb laser light, which in response causes an increase in the ablation rate and an increase in the spectral line intensity (Wang et al., 2018; Ahmed et al., 2021).

Table 2. Cu Plasma Parameters with Diffrent Laser Energy

Laser energy (mJ)	Te (eV)	$\times 10^{17}$ n_e (cm^{-3})	$f_p \times 10^{12}$(Hz)	$N_D \times 10^3$(cm^{-3})	$\lambda \times 10^{-5}$ (cm)
400	2.30	6.75	7.378	7.294	1.372
500	2.60	8.25	8.156	7.835	1.314
600	2.80	11.25	9.525	7.498	1.167
700	2.91	12.75	10.140	7.462	1.118
800	3	15.00	10.998	7.022	1.038

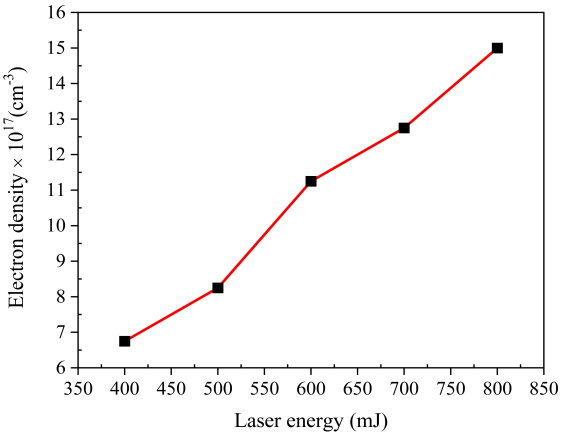

Figure 4. Cu Plasma Electron Density at Various Laser Energies

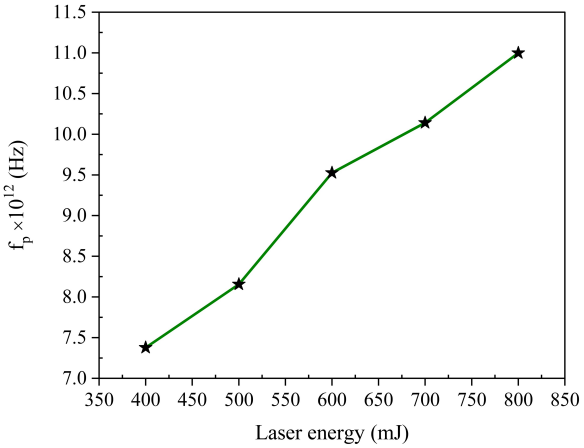

Figure 5. Plasma Frequency of Cu Plasma at Different Laser Energy

3.2 Fundamental Parameters of Cu Plasma

Laser-induced Cu plasma emits ionic and atomic spectral lines that may be used to measure properties of the plasma such as electron temperature (T_e) and electron density (n_e). The intensity ratio method of two spectral lines can be used to measure the temperature of the electrons in a plasma. The intensity ratio method uses two spectral lines that come from different upper levels of the same product and ionization level to measure the temperature of the plasma. Equation (1) represents the formula of the intensity two ratio method to measure electron temperature (Wainwright et al., 2020; Aadim et al., 2021):

$$\frac{I_1}{I_2} = \frac{g_1 A_1 \lambda_2}{g_2 A_2 \lambda_1} exp\left[-\left(\frac{E_1 - E_2}{K T_e}\right)\right] \quad (1)$$

Where: I_1, I_2, g_1, g_2, A_1, A_2, λ_1, λ_2, E_1, and E_2 represent the spectral lines' intensity, wavelength, statistical weight, transition probability, and energy for Cu spectral lines, respectively. T_e is the electron temperature, and K is the Boltzmann constant. Table (1) displays the relevant spectroscopic parameters for evaluating laser-produced Cu plasma transitions taken from the NIST atomic spectra database (Source: http://www.nist.gov/pml/data/asd.cfm).

Using the atomic spectral line (Cu I) at 570 nm and the ionic spectral line (Cu II) at 593.76 nm upon excitation at a wavelength of 532 nm, we were able to calculate the temperature of the plasma under the postulated local thermodynamic equilibrium (LTE) conditions. The Cu plasma electron temperature was determined depending on laser energy, ranging from 400 to 800 mJ. The value of the T_e range was (2.30-3) eV, as listed in Table (2). Figure 3 appear that the electron's temperature behavior increases as laser pulse energy increases. Due to plasma reflection and laser photon absorption, the plasma plume's electron temperatures rise when laser power is increased (Fikry et al., 2020; Ahmed et al., 2021).

The laser-produced Cu plasma's emission spectra showed broadened lines. Stark broadening, the primary effect on these emission spectra lines, is the result of collisions between the released charged particles and atoms; hence, the electron density may be determined from the spectral line widths and the Relation (2) (Suchoňová et al., 2017):

$$n_e(cm^{-3}) = \left(\frac{\lambda_{FWHM}}{2\omega}\right) \times 10^{16} \quad (2)$$

where: n_e is the electron density, λ_{FWHM} is the Stark full-width at half-maximum (FHWM), and ω is the electron impact

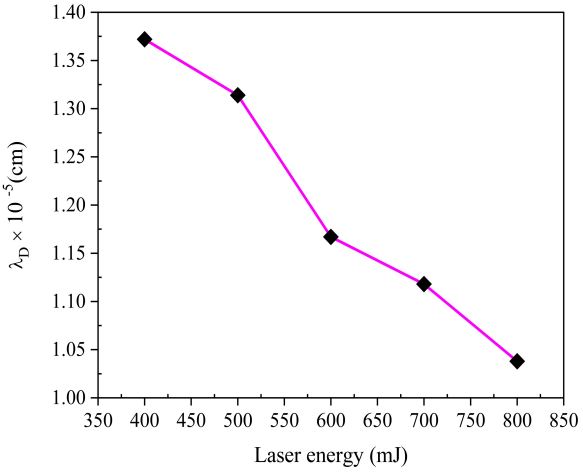

Figure 6. Cu Plasma Debye Length at Various Laser Energies

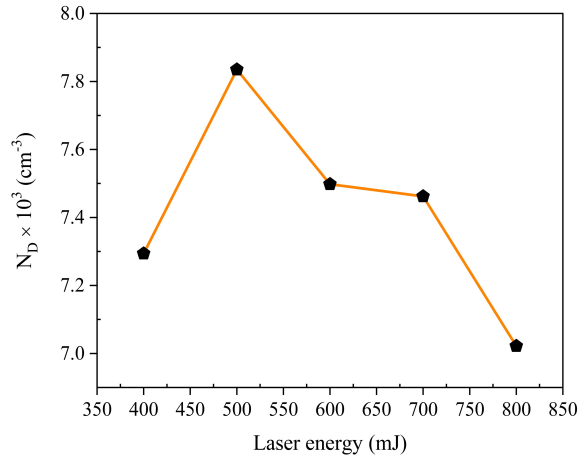

Figure 7. Cu Plasma Debye Number at Various Laser Energies

parameter.

Utilizing the spectral lines of Cu I at 570 nm, the electron density was calculated for different laser irradiation energies. The electron density value ranged from 6.75 to 15×10^{17} cm^{-3}, as reported in Table (2). Figure 4 indicates that when laser intensity increases, electron density increases, which is consistent with (Ahmed et al., 2021).

The findings demonstrated that electron density (n_e) and temperature (T_e) vary slowly or reach saturation. The observed phenomena may be explained by the plasma reflection of laser light, also known as the plasma shielding effect. When experiments are conducted at room temperature and pressure, the air acts as a barrier against the ionization process, reducing the available laser intensity for mass ablation.

3.3 Characterization of Other Basic Cu Plasma Parameters

To get a complete profile of the Cu plasma, we used electron temperature (T_e) and electron density (n_e) to measure the effect of laser energy on other basic plasma characteristics such as plasma frequency (f_p), particles in the Debye sphere (N_D), and Debye length (λ_D)

The equations representing these basic parameters (f_p), (N_D), and (λ_D) are given by Formulas (3), (4), and (5), respectively (Piel, 2010).

$$f_p = \left(\frac{n_e e^2}{\varepsilon_0 m_e}\right)^{\frac{1}{2}} \tag{3}$$

$$\lambda_D = \left(\frac{\varepsilon_0 k_B T_e}{n_e e^2}\right)^{\frac{1}{2}} \tag{4}$$

$$N_D = \frac{4\pi}{3}\lambda_D^3 n_e \tag{5}$$

where: ε_0, k_B, e, n_e, and m_e are the permittivity of free space, Boltzmann constant, charge of the electron, electron density, and mass of the electron, respectively.

The findings are summarized in Table (2), where it can be seen that when the laser energy was increased, f_p also increased. In contrast, both λ_D and N_D decreased when the laser energy was raised.

From Figure 5, we notice that the plasma frequency (f_p) increases with increasing laser energy. This behavior is due to more ablated material created with greater irradiation (Mohammed et al., 2022a).

It can be seen in Figure 6 that when the laser energy is raised, the Debye length (λ_D) decreases because the material absorbs more light. This finding is consistent with that of Aadim et al. (2021).

Figure 7 shows the number of particles in Debye's sphere (N_D) at a range of laser energies from 400 to 800 mJ. The findings correspond with those of (Mohammed et al., 2022a), who found that both N_D and λ_D exhibit comparable behavior as a function of laser energy because of their direct relationship.

4. CONCLUSION

Cu plasma characteristics were studied in relation to laser intensity. The optical emission spectrum, electron density, electron temperature, and other fundamental plasma parameters have been significantly impacted by varying the laser intensity. As the laser energy increased, there was a linear increase in the temperature of the electrons in the Cu plasma. Collisions between freed atoms and charged particles result in spectral line broadening proportional to the electron density. The mass ablation rate increased. linearly with laser intensity, resulting in a larger electron density.

5. ACKNOWLEDGMENT

The authors thank Dr. Aldes Lesbani, editor-in-chief of Science and Technology Indonesia, and reviewers of this paper for providing constructive comments to enhance the published version.

REFERENCES

Aadim, K. A., K. A. Ahmed, and R. S. Mohammed (2021). Diagnostic Analysis of Cu and Cuzn Plasma Produced by Nd: YAG Nanosecond Laser at 1064 nm. In *AIP Conference Proceedings*, volume 2372. AIP Publishing

Afgan, M. S., M. Anwar-ul Haq, S. Haq, M. Kalyar, and M. Baig (2018). Spectroscopic Investigations of the Laser Induced Thallium Plasma. *Laser Physics*, **29**(1); 016004

Ahmed, K. A., K. A. Aadim, and R. S. Mohammed (2021). Investigation the Energy Influence and Excitation Wavelength on Spectral Characteristics of Laser Induced MgZn Plasma. In *AIP Conference Proceedings*, volume 2372. AIP Publishing

Botto, A., B. Campanella, S. Legnaioli, M. Lezzerini, G. Lorenzetti, S. Pagnotta, F. Poggialini, and V. Palleschi (2019). Applications of Laser-Induced Breakdown Spectroscopy in Cultural Heritage and Archaeology: A Critical Review. *Journal of Analytical Atomic Spectrometry*, **34**(1); 81–103

Bulajic, D., G. Cristoforetti, M. Corsi, M. Hidalgo, S. Legnaioli, V. Palleschi, A. Salvetti, E. Tognoni, S. Green, and D. Bates (2002). Diagnostics of High-Temperature Steel Pipes in Industrial Environment by Laser-Induced Breakdown Spectroscopy Technique: The LIBSGRAIN Project. *Spectrochimica Acta Part B: Atomic Spectroscopy*, **57**(7); 1181–1192

Corsi, M., G. Cristoforetti, M. Hidalgo, S. Legnaioli, V. Palleschi, A. Salvetti, E. Tognoni, and C. Vallebona (2003). Application of Laser-Induced Breakdown Spectroscopy Technique to Hair Tissue Mineral Analysis. *Applied Optics*, **42**(30); 6133–6137

Fikry, M., W. Tawfik, and M. M. Omar (2020). Investigation on the Effects of Laser Parameters on the Plasma Profile of Copper using Picosecond Laser Induced Plasma Spectroscopy. *Optical and Quantum Electronics*, **52**; 1–16

Gupta, A., J. M. Curran, S. Coulson, and C. M. Triggs (2017). Comparison of Intra-Day and Inter-Day Variation in Libs Spectra. *Forensic Chemistry*, **3**; 36–40

Kasem, M. A., R. E. Russo, and M. A. Harith (2011). Influence of Biological Degradation and Environmental Effects on The Interpretation of Archeological Bone Samples with Laser-Induced Breakdown Spectroscopy. *Journal of Analytical Atomic Spectrometry*, **26**(9); 1733–1739

Keerthi, K., S. D. George, S. D. Kulkarni, S. Chidangil, and V. Unnikrishnan (2022). Elemental Analysis of Liquid Samples by Laser Induced Breakdown Spectroscopy (LIBS): Challenges and Potential Experimental Strategies. *Optics & Laser Technology*, **147**; 107622

Li, T., Z. Hou, Y. Fu, J. Yu, W. Gu, and Z. Wang (2019). Correction of Self-Absorption Effect in Calibration-Free Laser-Induced Breakdown Spectroscopy (CF-LIBS) with Blackbody Radiation Reference. *Analytica Chimica Acta*, **1058**(13); 39–47

Lorenzetti, G., S. Legnaioli, E. Grifoni, S. Pagnotta, and V. Palleschi (2015). Laser-Based Continuous Monitoring and Resolution of Steel Grades in Sequence Casting Machines. *Spectrochimica Acta Part B: Atomic Spectroscopy*, **112**; 1–5

Mohammed, R. S., K. A. Aadim, and K. A. Ahmed (2022a). Spectroscopy Diagnostic of Laser Intensity Effect on Zn Plasma Parameters Generated by Nd: YAG Laser. *Iraqi Journal of Science*, **63**(9); 3711–3718

Mohammed, R. S., K. A. Aadim, and K. A. Ahmed (2022b). Study the Effect of Fundamental and Second Harmonic Wavelength on Plasma Parameters of Emission Magnesium Lines in Nd: YAG Laser. In *AIP Conference Proceedings*, volume 2386. AIP Publishing

Piel, A. (2010). An Introduction to Laboratory, Space, and Fusion Plasmas. *Plasma Physics*; 35–40

Pyun, S. H., W. Min, B. Goo, S. Seit, A. Azzi, D. Y.-S. Wong, G. S. Munavalli, C.-H. Huh, C.-H. Won, and M. Ko (2023). Real-Time, in Vivo Skin Cancer Triage by Laser-Induced Plasma Spectroscopy Combined with a Deep Learning–Based Diagnostic Algorithm. *Journal of the American Academy of Dermatology*, **89**(1); 99–105

Radziemski, L. J. (2002). From LASER to LIBS, the Path of Technology Development. *Spectrochimica Acta Part B: Atomic Spectroscopy*, **57**(7); 1109–1113

Sancey, L., V. Motto-Ros, B. Busser, S. Kotb, J.-M. Benoit, A. Piednoir, F. Lux, O. Tillement, G. Panczer, and J. Yu (2014). Laser Spectrometry for Multi-Elemental Imaging of Biological Tissues. *Scientific Reports*, **4**(1); 6065

Shaikh, N. M., S. Hafeez, M. Kalyar, R. Ali, and M. Baig (2008). Spectroscopic Characterization of Laser Ablation Brass Plasma. *Journal of Applied Physics*, **104**(10)

Suchoňová, M., P. Veis, J. Karhunen, P. Paris, M. Pribula, K. Piip, M. Laan, C. Porosnicu, C. Lungu, and A. Hakola (2017). Determination of Deuterium Depth Profiles in Fusion-Relevant Wall Materials by Nanosecond LIBS. *Nuclear Materials and Energy*, **12**; 611–616

Tavares, T. R., A. M. Mouazen, L. C. Nunes, F. R. dos Santos, F. L. Melquiades, T. R. da Silva, F. J. Krug, and J. P. Molin (2022). Laser-Induced Breakdown Spectroscopy (LIBS) for Tropical Soil Fertility Analysis. *Soil and Tillage Research*, **216**; 105250

Wainwright, E. R., S. W. Dean, F. C. De Lucia, T. P. Weihs, and J. L. Gottfried (2020). Effect of Sample Morphology on the Spectral and Spatiotemporal Characteristics of Laser-Induced Plasmas from Aluminum. *Applied Physics A*, **126**(2); 1–18

Wang, J., X. Li, C. Wang, L. Zhang, and X. Li (2018). Effect of Laser Wavelength and Energy on the Detecting of Trace Elements in Steel Alloy. *Optik*, **166**; 199–206

Yamamoto, K. Y., D. A. Cremers, M. J. Ferris, and L. E. Foster (1996). Detection of Metals in the Environment using

a Portable Laser-Induced Breakdown Spectroscopy Instrument. *Applied Spectroscopy*, **50**(2); 222–233